

Manuscript Number: STOTEN-D-19-01104R1

Title: Effects of climate change on the design of subsurface drainage systems in coastal aquifers in arid/semi-arid regions: Case study of the Nile delta

Article Type: Research Paper

Keywords: sea level rise; coastal aquifer; climate change; subsurface draining systems; seawater intrusion

Corresponding Author: Dr. Andrea Scozzari, Ph.D.

Corresponding Author's Institution: CNR ISTI

First Author: Ismail Abd-Elaty, Ph.D.

Order of Authors: Ismail Abd-Elaty, Ph.D.; Gehan A.H. Sallam, Ph.D.; Salvatore Straface, Ph.D.; Andrea Scozzari, Ph.D.

Abstract: The influence of climate change on the availability and quality of both surface- and ground-water resources is well recognized nowadays. In particular, the mitigation of saline water intrusion mechanisms (SWI) in coastal aquifers is a recurrent environmental issue. In the case of the Nile delta, the presence of sea level rise (SLR) and the perspective of other human-induced stressors, such as the next operation of the GERD (Grand Ethiopian Renaissance Dam), are threats to be taken into account for guaranteeing resilient agricultural practices within the future possible scenarios. Subsurface draining systems can contribute to mitigate the vulnerability to climate change and to the increased anthropic pressure insofar they are able to receive the incremented flow rate due to the foreseen scenarios of SLR, recharge and subsidence. Subsurface drainage offers a practical solution to the problem of upward artesian water movement and the simultaneous downward flow of excess irrigation water, to mitigate the salinization in the root zone. This paper introduces a rational design of subsurface drainage systems in coastal aquifers, taking into account the increment of flow in the draining pipes due to future possible conditions of SLR, recharge and subsidence within time horizons that are compatible with the expected lifespan of a buried drainage system. The approach proposed in this paper is characterised by the assessment of the incremental flow through the drains as a function of various possible scenarios at different time horizons. Our calculations show that the impact on the discharge into the subsurface drainage system under the new foreseen conditions is anything but negligible. Thus, future climate-related scenarios deeply impact the design of such hydraulic structures, and must be taken into account in the frame of the next water management strategies for safeguarding agricultural activities in the Nile delta and in similar coastal contexts.

Response to Reviewers: First of all Authors want to express their gratitude to the Editor for the valuable comments and remarks.

1 **Effects of climate change on the design of subsurface drainage systems in coastal aquifers in**  
2 **arid/semi-arid regions: Case study of the Nile delta**

3 *Ismail Abd-Elaty<sup>1</sup>, Gehan.A.H.Sallam<sup>2</sup>, Salvatore Straface<sup>3</sup> and Andrea Scozzari<sup>4</sup>*

4  
5 <sup>1</sup>Department of Water and Water Structures Engineering, Faculty of Engineering, Zagazig University, Zagazig  
6 44519, Egypt.

7 <sup>2</sup>Drainage Research Institute (DRI), National Water Research Center (NWRC), Cairo, Egypt

8 <sup>3</sup> Department of Environmental and Chemical Engineering, University of Calabria, Ponte P. Bucci, 87036 Rende,  
9 Italy

10 <sup>4</sup>CNR Institute of Information Science and Technologies (CNR-ISTI), Via Moruzzi 1, 56024 Pisa, Italy,  
11 Email: a.scozzari@isti.cnr.it

12 **Keywords:** sea level rise, coastal aquifer, climate change, subsurface draining systems, seawater intrusion

13 **ABSTRACT:**

14 The influence of climate change on the availability and quality of both surface- and ground-water  
15 resources is well recognized nowadays. In particular, the mitigation of saline water intrusion mechanisms  
16 in coastal aquifers is a recurrent environmental issue. In the case of the Nile delta, the presence of sea  
17 level rise and the perspective of other human-induced stressors, such as the next operation of the Grand  
18 Ethiopian Renaissance Dam, are threats to be taken into account for guaranteeing resilient agricultural  
19 practices within the future possible scenarios. Subsurface drainage offers a practical solution to the  
20 problem of upward artesian water movement and the simultaneous downward flow of excess irrigation  
21 water, to mitigate the salinization in the root zone. Subsurface draining systems can contribute to mitigate  
22 the vulnerability to climate change and to the increased anthropic pressure insofar they are able to receive  
23 the incremented flow rate due to the foreseen scenarios of sea level rise, recharge and subsidence. This  
24 paper introduces a rational design of subsurface drainage systems in coastal aquifers, taking into account  
25 the increment of flow in the draining pipes due to future possible conditions of sea level rise, artificial  
26 recharge and subsidence within time horizons that are compatible with the expected lifespan of a buried  
27 drainage system. The approach proposed in this paper is characterised by the assessment of the  
28 incremental flow through the drains as a function of various possible scenarios at different time horizons.  
29 Our calculations show that the impact on the discharge into the existing subsurface drainage system under  
30 the new foreseen conditions is anything but negligible. Thus, future climate-related scenarios deeply  
31 impact the design of such hydraulic structures, and must be taken into account in the frame of the next  
32 water management strategies for safeguarding agricultural activities in the Nile delta and in similar  
33 coastal contexts.

## 1 Introduction

Climate change is a global phenomenon; however it's very variable on a geographical basis. It is defined as an imbalance in the usual climatic conditions such as heat, wind and rainfall patterns that characterize each region on earth. A number of phenomena is addressed to produce the sea level rise (SLR), and its acceleration that is currently observed, such as the thermal expansion of the oceans and seas, the melting of glaciers and ice caps including Greenland, and Antarctic ice sheets melting. According to the Intergovernmental Panel on Climate Change (IPCC, 2013), in year 2100 about 95% of the coastal areas in the world will be considerably affected by SLR, hence increasing the risk of inundation in internal land and salt water intrusion (SWI) in coastal aquifers (Agren and Svensson, 2017). Shaltout et al. (2015) indicated SLR effects in the Nile delta in terms of ongoing submergence. According to Sestini (1989) and IPCC (2008), Egypt is considered among the most vulnerable countries to the threat taken by SLR.

Recent measurements by both ground based and satellite observations also indicate an acceleration in the rates of SLR (Legeais et al., 2018). El Raey (2010) studied both environmental and socio-economical risks in the coastal zone of the Nile delta connected with climate change, also placing attention to SLR and subsidence. The IPCC in its 5<sup>th</sup> report (IPCC, 2013) predicts global SLR figures from 18 to 59 cm in the next 100 years. For what regards Egypt, such conditions would lead to the submergence of the low lying coastal zones and some parts of the Nile Delta adjacent to the northern coast. In addition to surface water issues, a particularly challenging aspect is the mitigation of saline water intrusion mechanisms (SWI) in groundwater, in the presence of sea level rise and with the perspective of other human-induced stressors, such as the next operation of the Grand Ethiopian Renaissance Dam (GERD), the overpopulation in the Nile delta and Nile valley, and the various forms of desertification processes currently observed (Aboel Ghar et al, 2004). The risk of increased salinization deeply impacts agricultural practices and must also be taken into account for the management of reclaimed lands.

The Nile delta aquifer is a Quaternary aquifer mainly composed of a Holocene clay cap layer and a series of Pleistocene layers (deepest confined aquifer). The Holocene clay cap acts as an aquitard in its southern part, with an average thickness between 5 and 25 m, while in the northern parts it acts as an aquiclude and its thickness is larger than 50 m (Said, 1962, 1981; Serag EI-Din, 1989). The Pleistocene layers consist of coarse-grained Quartzitic sands and gravels alternated by lenses of clay. Its thickness gradually increases

62 toward the sea, being about 200 m in the South and sometimes exceeding 950 m in the North (EI-  
63 Fayoumi, 1987; Said, 1993).

64 Both the risk of submergence and SWI are exacerbated by subsidence (Wöppelmann et al, 2013). Several  
65 mechanisms could be brought as cause of subsidence: the sediment loading and isostatic displacement, or  
66 the failure, faulting, and flow of under-consolidated sediments, the anthropogenic or tectonics factors and  
67 the sediment compaction. Analysing the scales, the patterns and the velocities observed across the  
68 northern Nile Delta, the sediment compaction is the only subsidence mechanism consistent with them.  
69 Rapid compaction rates have been recorded in the meter increment below the top 1.0 to 2.0 meters of  
70 sediment on the Nile Delta. These rates appear to decrease to around 5.0 to 6.0 meters in an irregular  
71 fashion and then continue to decrease more regularly to the base of the Holocene section (Stanley and  
72 Corwin, 2012). Much of the subsidence measured by previous studies occurs in conjunction with known  
73 Holocene sediment deposits. Therefore, subsidence patterns do appear to correlate with thick Holocene  
74 sediment accumulations, but also appear to be heavily influenced by young sediment deposits of less than  
75 3500 years old due to rapid compaction within the first few meters (Fugate, 2014).

76 Subsidence exhibits variable rates across the Nile delta (Becker and Sultan, 2009; Fugate, 2014), often  
77 higher than SLR. In particular, it is expected that vertical land motion has a relevant impact on the  
78 assessment of future scenarios and the relating time horizon, regarding the risks of both submergence and  
79 salt water intrusion. In particular, the combination of SLR and subsidence has an impact on the design of  
80 drainage systems, especially in view of an acceleration of both phenomena.

81 Laeven (1991) showed that the saline water of the Mediterranean Sea intrudes into the Nile aquifer at  
82 depths in the range from 175 to 225 m, in the deepest confined aquifer. Moreover, Sakr et al. (2004)  
83 analyzed the historical records from 1960 to 2000 and demonstrated the sensitivity of groundwater  
84 salinity with respect to the Nile flow and abstraction rates. Authors concluded that the reduction in the  
85 Nile flow and the extensive abstraction from the aquifer lead to an increase in groundwater salinity. The  
86 effect of Nile flow reduction, which is expected when the GERD will enter into operation (Abd-Elhamid  
87 et al., 2018), combined with the increased pumping of groundwater and the current trend of sea level rise

88 is expected to affect seawater intrusion mechanisms in the Nile Delta in a dramatic way, requiring the  
89 urgent identification and design of possible counter-measures.

90 Several studies were carried out on the Nile delta confined aquifer to investigate the possible impact of  
91 SLR, including Sherif and Al-Rashed (2001), Sherif et al. (2012), Sefelnasr and Sherif (2014), Abd-Elaty  
92 et al. (2014) and Abd-Elhamid et al. (2016). These studies indicated that SLR has a negative impact on  
93 saltwater intrusion, predicting a sure threat to a large quantity of freshwater. An alternative strategy to  
94 mitigate the SLR effects is the artificial recharge (AR). In the coastal aquifer it reduces the seawater  
95 intrusion growing the fresh water pressure in the aquifer. AR requires an increase of alternative water  
96 supplies, such as desalination plants and water reuse from one side and aquifer recharge systems on the  
97 other side (Abd-Elhamid and Abd-Elaty, 2017).

98 Drainage is an essential practice in agricultural irrigated lands for preventing water-logging and  
99 salinization (Abd-Elaty et al., 2010). When the conditions in an area are such that an upward seepage  
100 from an underlying aquifer occurs, the risks of water logging and salinity are more serious. Such  
101 conditions may prevail in some areas of the Nile delta. Especially the northern coast is expected to be  
102 negatively impacted by both SLR and subsidence in the future. Subsurface drainage offers a possible  
103 practical solution for avoiding the salinization of the ground in the root zone, in the presence of upward  
104 artesian water movement with a simultaneous downward flow of excess irrigation water.

105 The design objective of the drains is to keep the water table within specified limits, determining a flow of  
106 water through the soil to the drains. Bazaraa et al. (1986) studied the artesian and anisotropic effects on  
107 drain spacing. Subsurface drainage systems installed in a soil overlying an artesian aquifer should be  
108 designed to handle both the upward artesian water flow and the downward seepage flow due to irrigation  
109 and rainfall. Proper drain spacing and sizing depends on several parameters, and it is known that drains  
110 subject to artesian conditions require a narrower spacing with respect to the simplest condition  
111 characterized by downward seepage only.

112 In 2011, Kalantari studied the impact of climate change on drainage systems. The study concluded that  
113 hydrological models are fundamental tools to assess the discharge dynamics, and the expected changes  
114 due to climate factors. Deelstra (2015) indicated that drainage construction is often carried out based on

115 existing practice and experience. Today, this might not be suitable under conditions of climate change,  
116 anthropic pressure and increased extreme events. Therefore, factors of influence on the design of drainage  
117 systems should be known and taken into account. A deep understanding of the interaction between  
118 climate, geological setting, land use, watershed hydrology and groundwater flow is a necessary  
119 prerequisite for the design of a draining system characterized by a long-enough service time horizon.

120 The design improvement of drainage systems according to new perspective scenarios characterized also  
121 the recent literature related to the North American region. In 2017, Pease et al. used the DRAINMOD  
122 hydrologic model to simulate the expected climate change effects on subsurface drainage and the  
123 performance of controlled drainage in the western Lake Erie Basin (US), where the climate change is  
124 expected to increase both annual rainfall and temperatures. The study indicated that the development of  
125 strategies to mitigate the impact of these changes is important for ensuring agricultural resiliency to the  
126 future climate. British Columbia (Canada) Agriculture & Food Climate Action Initiative (2013) reported  
127 that, in the countries where subsurface drainage is necessary, a proper design of drainage systems must  
128 take into account the mitigation of risks related with the climate change.

129 The adaptation of drainage systems design to climate change varies greatly depending on local conditions,  
130 in Egypt most of the previous studies did not take into account the effect of climate change on subsurface  
131 drainage design, neither the effect of subsidence was considered. This paper represents a first building  
132 block for the proper design of subsurface drainage (SD) systems in the Nile delta and in coastal aquifers  
133 in general, in the presence of multiple climate-related forcing parameters. In particular, attention is  
134 focused on SLR, subsidence, and on the artificial subsurface recharge that is hypothesized in order to  
135 reduce the aquifer salinity.

136 This paper introduces a rational design of subsurface drainage systems in coastal aquifers, by estimating  
137 the flow in the draining pipes and its possible increment due to the foreseen scenarios of SLR, recharge  
138 and subsidence. A novel approach proposed in this paper consists in the assessment of the incremental  
139 flow through the drains as a function of various possible scenarios. The next sections will illustrate the  
140 assumptions made and the methods used to build the scenarios, and the evaluation of the expected impact  
141 on the design of subsurface drainage systems.

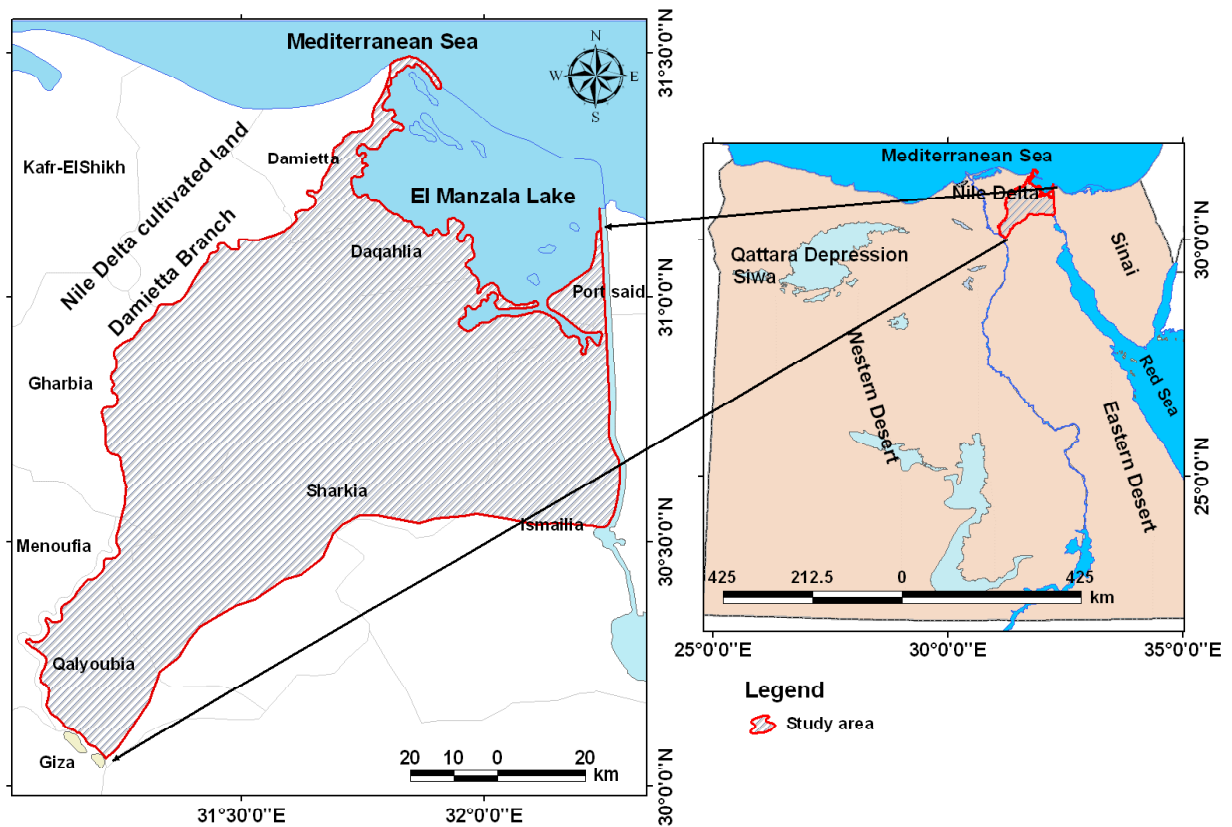
142

143 **2 Materials and Methods**

144 **2.1 Eastern Nile Delta Aquifer (Case Study Area)**

145 The Eastern Nile Delta aquifer was selected as a case study area to perform the numerical simulations.  
146 The study area is bounded by the Damietta Branch at the West, El Manzala Lake at the North, Ismailia  
147 Canal at the South and Suez Canal at the East, and its size is about 9500 km<sup>2</sup>. It is located between  
148 latitudes 31° 00' and 32° 30' N, and longitudes 29° 30' and 32° 30' E, as shown in Figure 1 (Nosair, 2011).

149 The aquifer system of the Nile Delta is one of the largest in the world for its areal extension and layer  
150 thickness, with a total capacity of about 500 Bm<sup>3</sup> (Sherif, 1999). Its characteristics have been identified  
151 by numerous studies, assuming that it's formed by quaternary deposits and considered a semi-confined  
152 aquifer as a whole (Al Agha, 2015). The geology of the aquifer includes Quaternary deposits of Holocene  
153 and Pleistocene sediments, plus Tertiary deposits including the Pliocene, Miocene, Oligocene, Eocene,  
154 and Paleocene sediments. The Quaternary aquifer thickness ranges from 100 m in the South, near Cairo,  
155 to nearly 1,000 m at the coast of the Mediterranean Sea (RIGW, 1980). The hydrological strata are  
156 composed of sands and gravels (Pleistocene and Holocene) containing few lenses of clays. These are  
157 considered the main water-bearing formations (Sherif et al., 2012). The Quaternary base is a clay  
158 aquiclude with a slope of about 4 m/km, which is about 40 times the ground surface slope (Serag EIDin,  
159 1989; Said, 1993), as shown in Figure 2. A number of studies were carried out on the Nile Delta aquifer  
160 system under different scenarios of pumping rate (Sherif and Al-Rashed, 2001). In general, the most  
161 permeable layer has been found at depths between 55 and 150 meters from the land surface (Sefelnasr and  
162 Sherif, 2014).



163

164

Figure 1: Location map of the East Nile Delta aquifer (from Nosair, 2011)

165

166

167

168

169

170

171

172

173

174

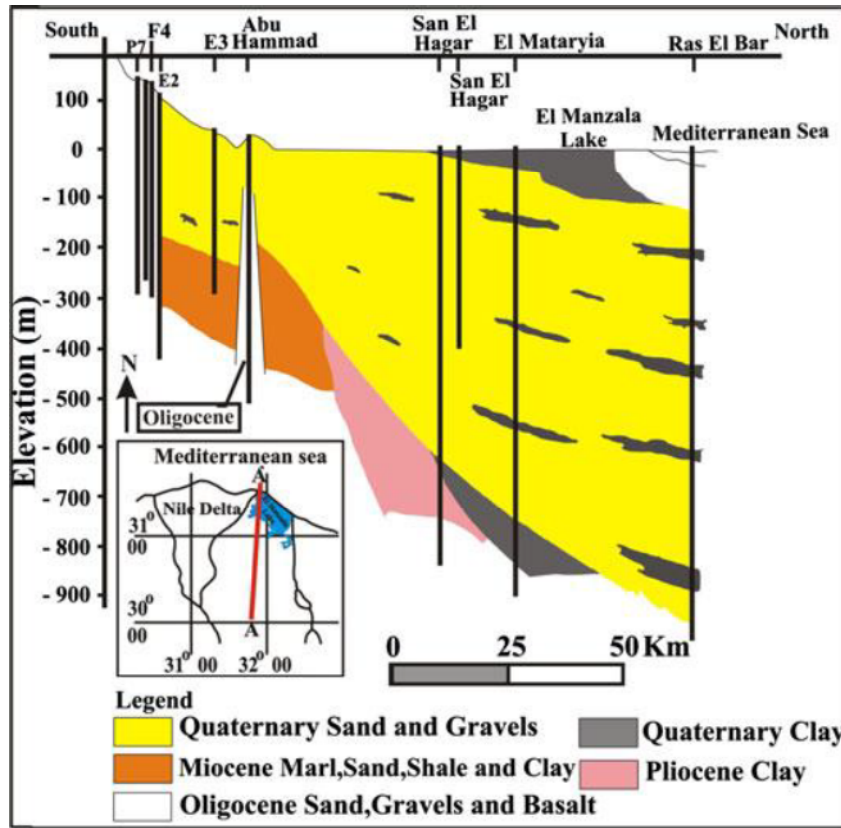
175

176

177

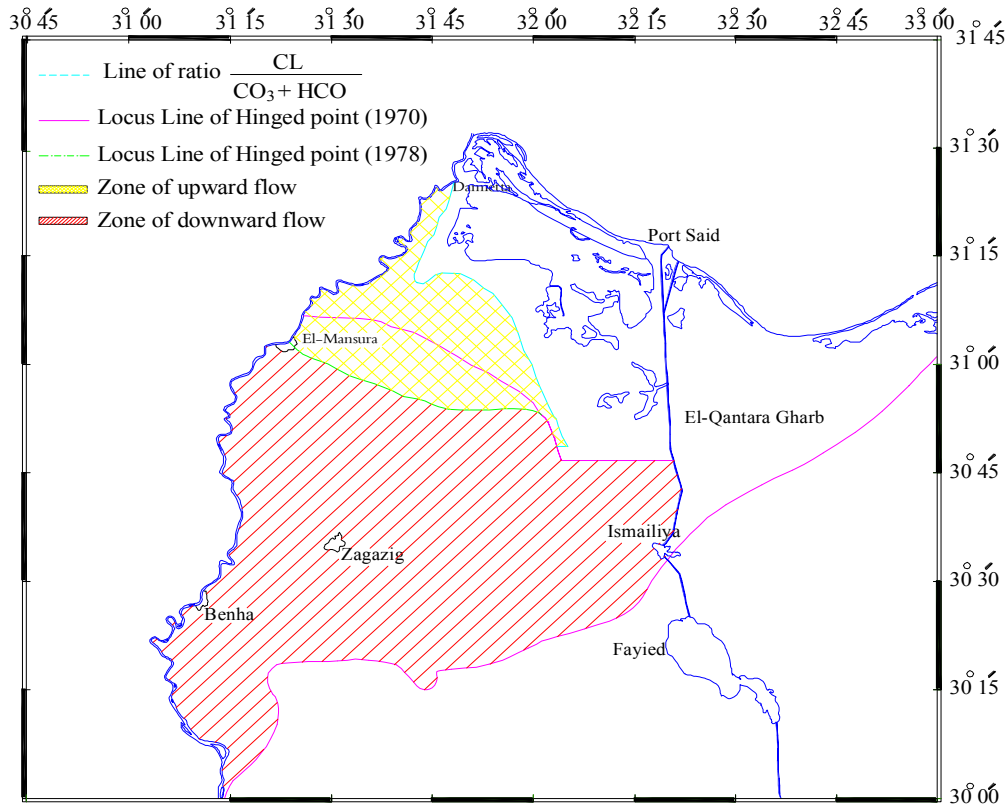
178

According to the field data compiled and processed by RIGW (1980), the top soil layer consists of clay, with a thickness that varies generally from 40 m in the North, middle and West Delta region, to about 90 m that are reached at the Damietta branch, with a general increment from West to East. So, according to the thickness of the clay layer, the semi-pervious clay cap admits leakage from the deepest to the shallow aquifer. The northern part of the aquifer is subject to upward flow, due to the difference in head of these water bodies that causes vertical movement of groundwater in the clay cap as shown in Figure 3. The quantity of upward flow in the delta aquifer is almost  $50 \times 10^6 \text{ m}^3/\text{year}$  (Faried, 1979). On the other hand, the main aquifer is recharged by means of the irrigation canals, the seepage from the Damietta branch in Southwest and Ismailia Canal in the Southeast, plus the irrigation water excess. The latest estimates point out an amount of recharge deriving from irrigation practices of about 0.54 mm/day, while the average water loss by evaporation is around 311 mm/year (RIGW/IWACO 1990). According to different estimated depths of the groundwater table (reported by RIGW, 2002 and Morsy, 2009) the depth of the groundwater table in this aquifer ranges between 1- 2 m in the North, 3– 4 m in the center and 5 m in the South.



179

180 Figure 2: Longitudinal cross-section showing the thickness and litho-facies variation of the Quaternary  
 181 aquifer in Nile Delta (from El Fayoumy, 1968)



182

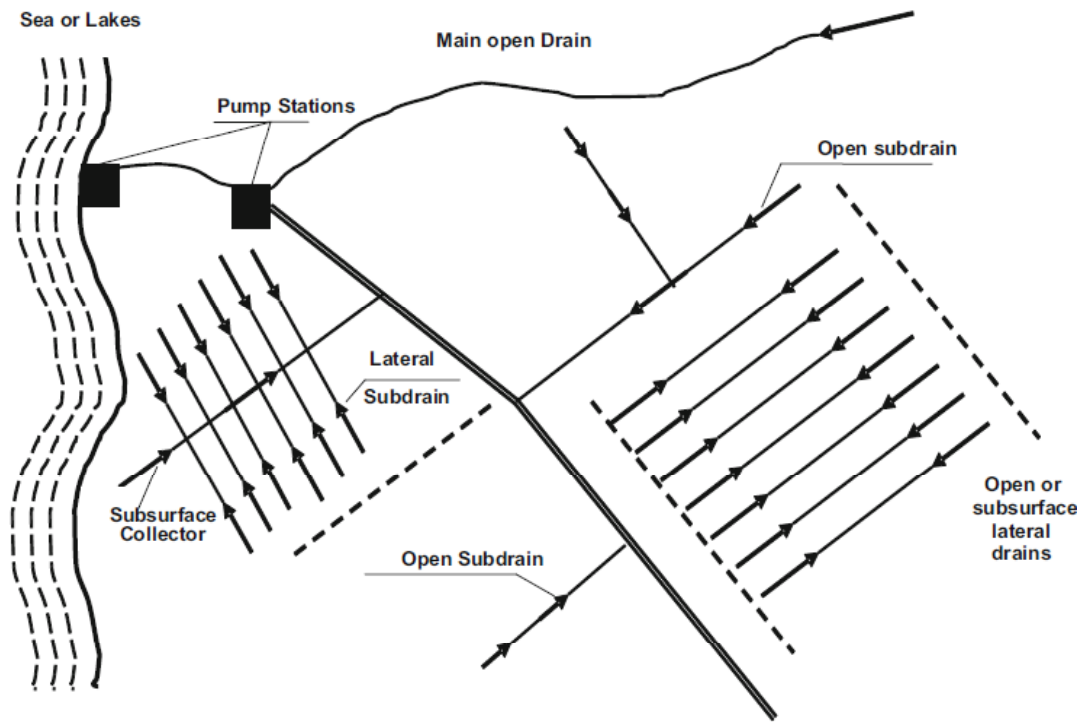
183 Figure 3: Locus line of the hinge points separating the upward and downward flow zones (After Amer,  
 184 1981)

185  
186 Morsy (2009) estimated the total annual groundwater abstraction in the Nile Delta area to be 4.9 Bm<sup>3</sup> in  
187 2008, for irrigation and drinking purposes. The abstraction rate increases linearly by about 0.1 BM<sup>3</sup> per  
188 year, except the period from 2003 till 2010 by rate of 0.2 BM<sup>3</sup> per year (Sallam, 2018). In the study area  
189 of this paper (the eastern Delta) the amount of groundwater used in agriculture is about 326 Mm<sup>3</sup>/year  
190 (Abu-Zeid, 1991) while the total amount reached 1.38 Bm<sup>3</sup> in 2008. The main contributions to  
191 groundwater discharge are represented by subsurface drainage and overexploitation of the aquifer.  
192 According to Fawzi & Kamel (1994), the groundwater is discharged into the drainage system at a rate of  
193 1.0 mm/day in all the northern (coastal) part of the Nile delta.

194 In 1979, Atta analyzed the salinity of groundwater in the Nile delta based on the sampling of 50 wells,  
195 finding values between 227 ppm and 15264 ppm. The salinity generally increases towards the  
196 northeastern zone, while the northern parts and the areas adjacent to the Nile River canals have lower  
197 salinity. Farid (1980, 1985) presented maps of salinity distribution, where iso-salinity lines in terms of  
198 total dissolved salts (TDS) range from 640 to 45,000 ppm, and vertical cross sections with iso-salinity  
199 lines (TDS) ranging from 1,000 ppm to 35,000 ppm. These results agreed with (Atta, 1979) and indicated  
200 that the northern zone is highly saline due to saltwater intrusion. Morsy (2009) analyzed and presented the  
201 groundwater salinity from 1960 to 2008 based on historical groundwater quality data taken from the  
202 literature and from the Research Institute for Groundwater of the Egyptian National Water Research  
203 Center (RIGW ) database for wells at depths from 30 to 135 m. These analyses confirmed the results  
204 shown by Sakr et al. (2004), i.e., the depths at which higher groundwater salinity was found confirm the  
205 existence of a clay layer with low permeability over the deepest confined aquifer. Such clay cap is above  
206 the depths where Laeven (1991) found the intrusion of saline water. Interestingly, Sherif et al. (2012),  
207 Abd-Elaty et al, (2014) and Abd-Elhamid et al, (2016) simulated and described that the seawater in the  
208 Nile aquifer migrated to a distance range from 48 to 76.25 km and from 72.50 to 93.75 km from the  
209 shoreline for the iso-salinity lines (TDS) at 35000 ppm and 1000 ppm, respectively.

210 The surface water network (Nile branches, drains and irrigation canals) has a fundamental function to  
211 determine the hydrogeological conditions in the northern part of the East Nile Delta area. The subsurface  
212 drainage system protects the irrigated soils against salt accumulation and enables recycling of the

213 irrigation water. It consists of an extensive drainage network of field drains, sub-collectors, collectors and  
214 main drains (Figure 4), which either convey the drainage water back to the Nile, or discharge into coastal  
215 or inland lakes or directly to the sea (MWRI, 2013).



216

217 Figure 4: Schematic diagram of Nile delta surface and subsurface drainage networks

218

## 219 2.2 Description of the Numerical Model

220 The numerical model used to simulate the seawater intrusion in the Nile delta aquifer is based on the  
221 assumption of phreatic coastal aquifer subject to a top-down infiltration due to recharge (rainfall plus  
222 irrigation) and a bottom-up flow through a confined aquifer.

223 Seawater intrusion phenomenon is a miscible variable density process governed by the following coupled  
224 system of flow and transport equations:

$$\begin{aligned} \phi \frac{\partial \rho}{\partial t} - \nabla \left( \frac{\rho \mathbf{K}}{\mu} (\nabla p + \rho g \nabla z) \right) &= 0 \\ \phi \frac{\partial (\rho C)}{\partial t} + \nabla (\rho \mathbf{q} C) - \phi \nabla (\rho \mathbf{D} \nabla C) &= 0 \end{aligned}$$

225 (1)

226 where  $\mathbf{K}$  is the hydraulic conductivity tensor;  $p$  is pressure;  $\phi$  is porosity;  $\rho$  and  $\mu$  respectively are fluid  
 227 density and viscosity;  $g$  is the gravitational constant;  $C$  is the solute (salt) concentration;  $\mathbf{D} = (\phi d + \alpha_T |\mathbf{v}|) \mathbf{I}$   
 228  $+ (\alpha_L - \alpha_T) \mathbf{v} \mathbf{v}_T / |\mathbf{v}|$  is the hydrodynamic dispersion tensor and  $d$  diffusion coefficient;  $\alpha_T$  and  $\alpha_L$   
 229 respectively are transverse and longitudinal dispersivity;  $\mathbf{v} = \mathbf{q} / \phi$  is the fluid velocity, and the superscript  
 230  $T$  denotes transpose. System (1) is closed by specifying a constitutive relationship,  $\rho = \rho_f + \beta C$ , where  $\beta =$   
 231  $(\rho_s - \rho_f) / C_s$ ,  $\rho_s$  and  $\rho_f$  being salt and freshwater density respectively, and  $C_s$  the saltwater concentration.

### 232 2.2.1 Regional scale numerical model: Seawater intrusion in the Nile delta aquifer

233 The latest version of SEAWAT (Langevin et al., 2008), a coupled version of MODFLOW and MT3DMS  
 234 to integrate the density-dependent flow and the solute transport equation, was used to simulate seawater  
 235 intrusion in the Nile delta aquifer at a regional scale.

236 Subsurface flow and solute transport in the main aquifer was modelled by using 160 rows and 124  
 237 columns of active cells, with a cell dimension of  $1.0 \times 1.0 \text{ km}^2$ . The Nile Delta aquifer was divided into  
 238 eleven layers. The first layer represents the clay cap with depth varied between 20 m in the North to 50 m  
 239 in the North. The other layers, which represent the Quaternary aquifer, were divided into slices of equal  
 240 thickness, until an average depth of 200 m near Cairo to a depth of 1000 m at the coast line.

241 A constant head boundary condition was set equal to zero at the northern boundary along the shore line,  
 242 also at the western boundary a fixed head was imposed, between 16.15 m at the North and 0.25 m at  
 243 North. On the other hand, the domain is bounded to the South by the Ismailia canal, with a variable water  
 244 level between 16.15 m at its westernmost point and 7.00 m at its easternmost point, so a Dirichlet  
 245 boundary condition was assigned. The East boundary was considered impermeable and a no-flow  
 246 (Neumann) boundary condition was set. During the simulation, the hydraulic head boundaries along the  
 247 Nile branches were assumed as constant. The hydrodynamic parameters fed to the model are shown in  
 248 Table 1.

249

250

251 **Table 1:** Summary of hydraulic parameters used as an input to the model

<b>Hydraulic Parameters</b>	<b>Value</b>
Vertical Quaternary hydraulic conductivity $K_v$ (m/d)	0.50 - 10
Horizontal Quaternary hydraulic conductivity $K_h$ (m/d)	5 - 100
Vertical clay cap hydraulic conductivity $K_v$ (m/d)	0.01 - 0.025
Horizontal clay cap hydraulic conductivity $K_h$ (m/d)	0.10 - 0.25
Porosity	0.25 – 0.40
Longitudinal dispersivity ( $\alpha_L$ ) (m)	250
Transversal dispersivity ( $\alpha_T$ ) (m)	25
Diffusion coefficient (d) ( $m^2/day$ )	$10^{-4}$
<b>Hydraulic Forcing</b>	<b>Value</b>
Recharge (mm/day)	0.25 - 0.80
Total abstraction ( $m^3/year$ )	$2.78 \times 10^9$

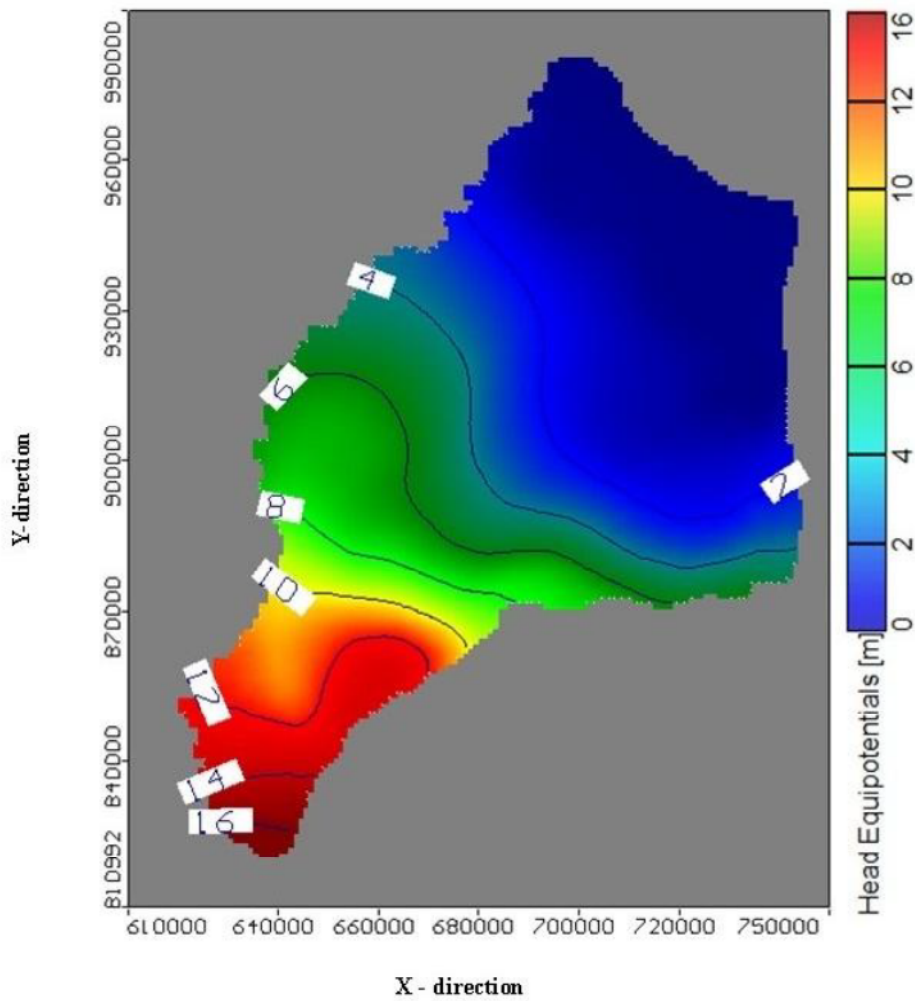
252

253 In order to obtain realistic results, the numerical model of the Nile Delta aquifer was calibrated by using  
 254 available historical records, consisting in hydraulic head measurements in a number of piezometers  
 255 distributed in the studied area, during a field campaign in 2008 (RIGW). The calibration of the numerical  
 256 model was based on the comparison between modeled and measured hydraulic heads, by modifying the  
 257 values of hydraulic conductivity, of porosity and of aquifer recharge rate, in order to optimize the match  
 258 between the modeled and observed heads.

259 After calibration of the model, the maximum difference between measured and modeled heads (ranging  
 260 from 16.00 to 0.0 respectively), is about 10 %, corresponding to about 1.60 m in the southernmost point.  
 261 Comparing the calculated heads with the observed measurements in the Nile delta aquifer, the root mean  
 262 square (RMS) of the residuals was equal to 0.329 m with a residual range between -0.215 and 0.488 m  
 263 and a normalised RMS of 2.744 % (i.e. normalized with respect to the maximum difference in the  
 264 observed head values). The results of the numerical model, in terms of hydraulic head (Figure 5), are in  
 265 good agreement with the observed heads described in RIGW (2008).

266 A transport model has also been used to determine sea water intrusion (SWI) in the Eastern Nile delta  
 267 aquifer. Firstly, it was calibrated by using field data of saltwater intrusion published by Sherif et al.  
 268 (2012). The hydrodispersive parameters (i.e.  $\alpha_L$  and  $\alpha_T$ ) contained in equations (1) have been calibrated by

269 comparing saltwater concentrations measured by Sherif et al. (2012) with modeled concentrations.  
270 Calibration results are presented in Figure 6, which shows the distribution of total dissolved salts (TDS)  
271 in the middle of the aquifer (layer #6), assigning an average thickness of 450 m at the North and 100 m at  
272 the South. These values are in good agreement with the field data of SWI in the Nile delta aquifer by  
273 Sherif et al (2012). The isochlorine at 35000 ppm reaches a distance of 75.85 km from the shoreline,  
274 while the isochlorine at 1000 ppm reaches a distance of 90.40 km.



275

276

Figure 5: Map of calculated groundwater head (simulation model) in the studied aquifer

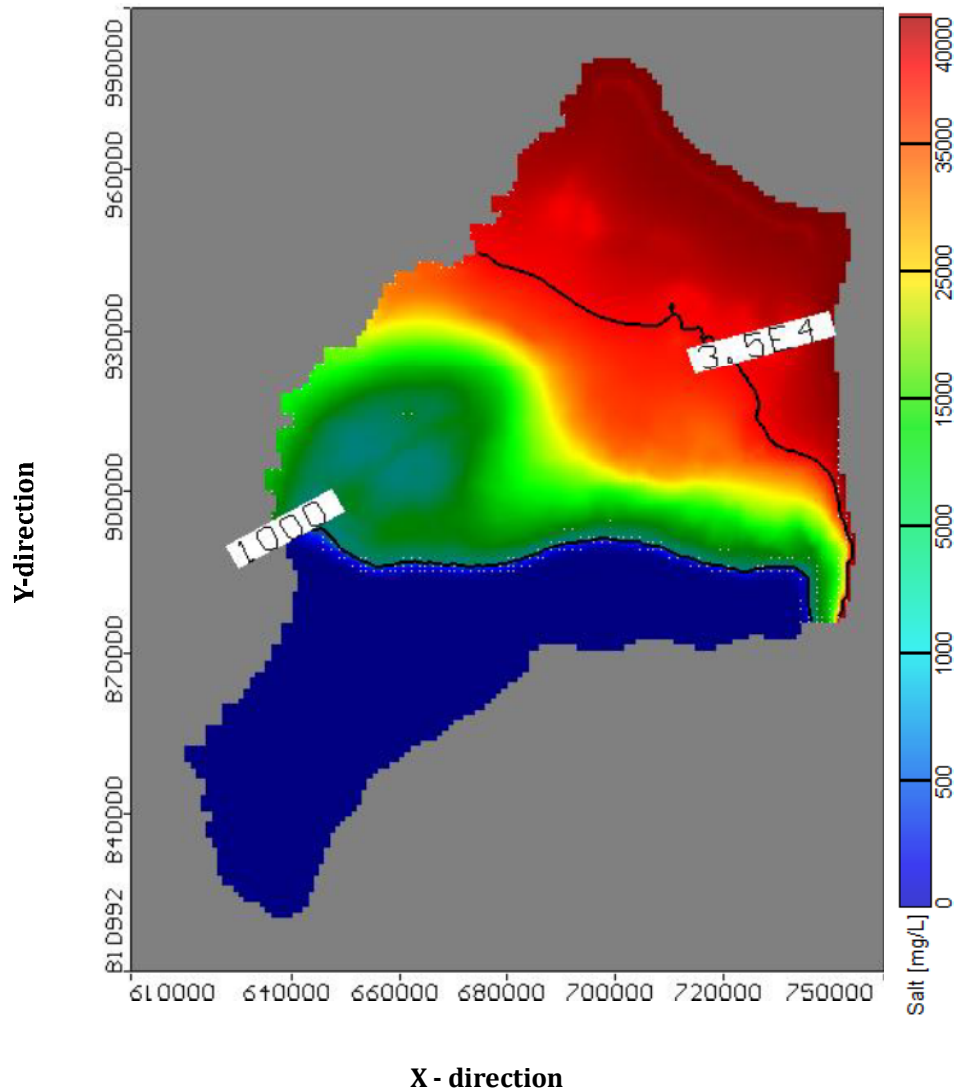


Figure 6: Map of TDS (output by SEAWAT) in the studied aquifer

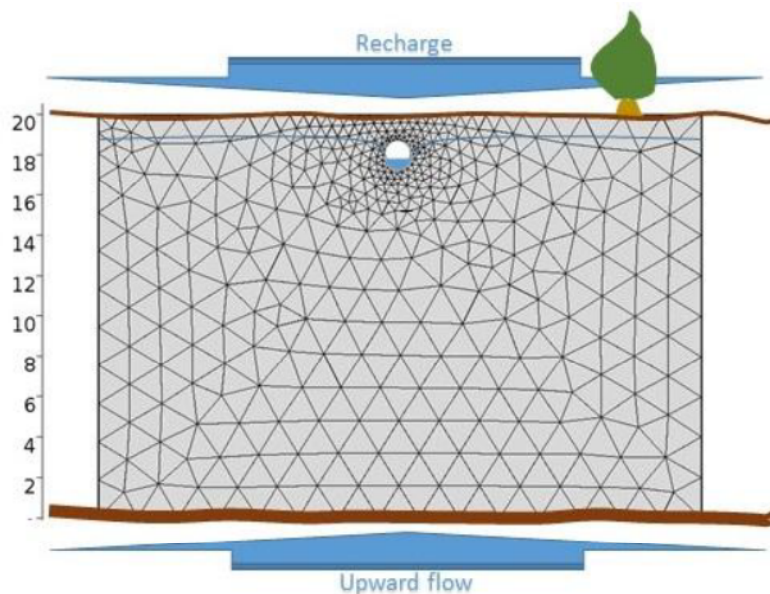
### 2.2.2 Local scale numerical model: subsurface drain discharge

In some areas of the Nile delta, especially in the North, the risk of water logging and salinisation due to the upward seepage from the underlying aquifer is very serious. Subsurface drainage systems, installed in the soil overlying artesian aquifers, offer a practical solution to the problem of upward artesian (brackish) water movement. The drain size and spacing need to be properly calculated (Abdel-Dayem, 1984) to make the drainage system able to discharge the excess of irrigation water as well as the upward groundwater flow. In practice, subsurface drains must be designed to withstand the necessary water flow, which permits to tie the water table to the required depth, for any foreseen working condition that may happen within the lifetime of the hydraulic structure. Thus, in the particular case of the Nile delta and of coastal aquifers in general, the SD design must take into account the effects of SLR, subsidence, and all

289 the human actions on the groundwater flow (e.g. over-pumping, surface flow reduction, artificial  
290 recharge, etc.). This is a mandatory effort to be done, in order to guarantee resilience of agricultural  
291 practices towards possible climate change scenarios. It must be noted that this effort has been  
292 substantially underestimated until today.

293 The hypothesized geometry for the draining system considered in this study consists in a series of  
294 identical parallel drains, regularly distributed with an equal spacing distance, orthogonal to a main  
295 collector.

296 A Finite Element Model was implemented in the COMSOL Environment (COMSOL, 2008) in order to  
297 simulate the response of the subsurface drainage system to the actions of SLR, artificial recharge and  
298 subsidence. The numerical model has a domain size of  $20.0 \times 30.0 \text{ m}^2$  discretized with 5000 irregular  
299 elements (Figure 7). The main hydrological parameters used for the simulation of the drain system  
300 geometry are the hydraulic conductivities ( $K_h = 1.83 \times 10^{-6} \text{ m/s} = 10 \times K_v$ ) and the porosity ( $\phi = 0.3$ ). The  
301 main forcing acting on the model is the hydraulic head variation  $\Delta G$  (cm) observed at the drain level due  
302 to SLR, recharge increment and subsidence.



303  
304 Figure 7: Design criteria of the drainage system at an artesian aquifer  
305

306 This model is used to calculate how the flow rate into the drains is modified by different working  
307 conditions, linked to the said climate-related scenarios, for the fixed geometry (in particular, given the  
308 distance between adjacent drains and their underground depth). By analyzing a set of possible future

309 combinations of SLR, subsidence and recharge within the next tens of years, useful estimations for an  
310 optimal performance of the drainage system can be done.

### 311 **2.3 SLR datasets**

312 The estimation of SLR is carried out by analyzing the time series of tide gauge measurements (sometimes  
313 longer than 100 years), which are today completed by satellite radar altimetry measurements (about 25  
314 years of global data at the time of writing this paper). The combination of advanced radar altimetry  
315 techniques, GPS and Synthetic Aperture Radar (SAR) interferometry with the persistent scatterer  
316 technique (Crosetto et al, 2016), permits to cross-validate such challenging measurements and separate  
317 the contributions of SLR and vertical land motion (VLM) to tide gauge measurements.

318 For what regards the mere SLR estimation on the coasts of the Nile delta, Essink and Kleef (1993)  
319 indicated 60 cm as a reasonable estimate within a time horizon of 100 years. The current estimation of the  
320 average global SLR derived from satellite altimetry is about 3.3 mm/year with an acceleration of 0.1  
321 mm/y<sup>2</sup> (Legeais et al., 2018), and it's very variable on a geographical basis, as stated by the ESA Sea-  
322 Level CCI (Climate Change Initiative) project (ESA SL-CCI, 2018). Actually, one of the main issues of  
323 satellite radar altimetry lies in the extraction of accurate sea level estimations when approaching the  
324 coasts (Vignudelli et al., 2011). In the absence of a global coastal sea level product, near-shore  
325 measurements at the northern coasts of the Nile delta would require a specific study, which falls outside  
326 the scope of this paper. Instead, gridded data of global mean sea level (for open ocean studies) have  
327 already been produced by the altimetry community and can be used for rough estimates, provided that  
328 datapoints closest to the coasts are usually few km off the shoreline (the spatial resolution is 1/4 of  
329 degree). Based on the regional mean sea level trend map published by the CCI project, the SLR in front of  
330 the Nile delta coasts can be roughly estimated in 4 mm/year. A deeper discussion of SLR rate and  
331 acceleration, with an adequate approximation for the purpose of this paper, is provided in Section 3.1.

332

### 333 **3 Results and Discussion**

#### 334 **3.1 The effect of SLR and recharge on the coastal aquifer and its quantification**

335 The objective of this section is to estimate the effects of a hypothetical future SLR on the piezometric  
336 head and its impact on the SD system by means of the regional numerical model. All the following  
337 evaluations are made in terms of foreseen scenarios used to determine the hypothesized inputs to the  
338 numerical models. Thus, hypotheses are done for a structure built in year 2000 (taken as a time  
339 reference), and scenarios are calculated relating to years 2020, 2040 and 2060, in order to better  
340 understand the possible impact of such phenomena within a time horizon compatible with the life  
341 expectancy of the buried draining structure..

342 SLR values for the three time horizons selected were determined according to the most recent available  
343 information at the time of writing this paper. Being the fundamental aspects of SLR estimation already  
344 introduced in Section 2, here we briefly discuss the reasoning behind the values fed as an input to the  
345 modelling exercise.

346 A constant SLR rate has been assigned to the eastern shoreline of the Nile delta, by averaging selected  
347 grid points from the sea-level CCI data base (ESA SL-CCI, 2018), which estimates mean sea level  
348 variations by combining multiple satellite altimetry missions. By averaging the closest grid points to the  
349 interested shoreline (7 points total) we obtained an SLR rate of 3.20 mm/yr. The cited SL-CCI data are  
350 referred to year 2016, thus, cumulated mean sea level variations with respect to year 2000 (for the  
351 selected years 2020, 2040 and 2060) were calculated by introducing an additional acceleration to the said  
352 SLR rate. The most updated global SLR acceleration rate is calculated in (Nerem et al., 2018), where the  
353 authors estimate a “climate-change–driven” acceleration of 0.084 mm/y<sup>2</sup>.

354 Based on these assumptions, SLR values of 5.7 cm, 14.5 cm and 26.7 cm (referred to year 2000) were  
355 estimated for the years 2020, 2040 and 2060, respectively.

356 The results of the regional numerical model show an advancement of the sea water intrusion (SWI) in all  
357 three cases. Specifically, the isochlorine at 35000 ppm reaches a distance from the shoreline of 76.25 km,  
358 76.50 km and 77.05 km respectively (it was 75.85 km in year 2000), while the isochlorine 1000 ppm  
359 reaches a distance of 90.60 km, 90.75 km and 90.85 km, respectively. These results confirm that SLR

360 leads to increase SWI in the whole aquifer with a southbound propagation, thus carrying an increased  
 361 salinity of the water and soil in the root zone, which is negatively impacting the crop productivity starting  
 362 from the coastal areas. The salt volume in the Eastern Nile Delta aquifer reaches  $3.1288 \times 10^{13}$ ,  
 363  $3.124937 \times 10^{13}$ ,  $3.123316 \times 10^{13}$ , and  $3.2116832 \times 10^{13}$  Kg for a SLR of 0 cm, 5.7 cm, 14.5 cm and 26.7 cm,  
 364 respectively. The percentages of aquifer salt volume were increased by 1.50%, 2% and 4%, confirming  
 365 that SLR leads to increase the salt volume in the aquifer.

366 An artificial recharge scheme is thus hypothesized, in order to counteract the incremented SWI due to  
 367 SLR. To do that, the approach followed in this research applies a recharge upstream the Nile delta (i.e., in  
 368 its northern part) at variable percentage rates. This permits to foresee more complete and effective  
 369 scenarios for the future design of subsurface draining systems and for the assessment of the draining  
 370 systems that are currently active. A total of 9 runs of the regional model were carried out, in order to  
 371 simulate all the combinations between SLR and the proposed recharge rates to control the SWI.

372 Table 2 summarises the model results, taking into account both the expected SLR and 3 possible recharge  
 373 scenarios, calculated in order to have an inversion of the intrusion process with the lowest value of  
 374 recharge. The results in terms of intrusion length and aquifer salt volume (where  $C_0$  is the initial salt  
 375 concentration and  $C$  is the salt concentration at the given combination of SLR and recharge) are also  
 376 shown in Table 3.

377 The table presents the percentage (%) of recharge required to keep the intrusion at the base case for three  
 378 cases of SLR so the percentage of required recharge are 1, 1.50 and 3% at SLR of 5.70, 14.50 and 26.70  
 379 cm while the intrusion reached 90.34, 90.36 and 90.34 for the isochlorine 1000 ppm while it reached  
 380 75.79, 75.82 and 75.75 ppm for the isochlorine 35000 ppm. Also the aquifer salt variation  $(C-C_0)/C_0$  were  
 381 calculated to check the aquifer salt situation which the positive sign indicated that the aquifer salt is more  
 382 than the base case and this is a negative impact to salt remove while the negative sign represents the  
 383 recharge have a positive effect on saltwater intrusion.

384 **Table 2:** Regional model results as a function of SLR and various recharge levels

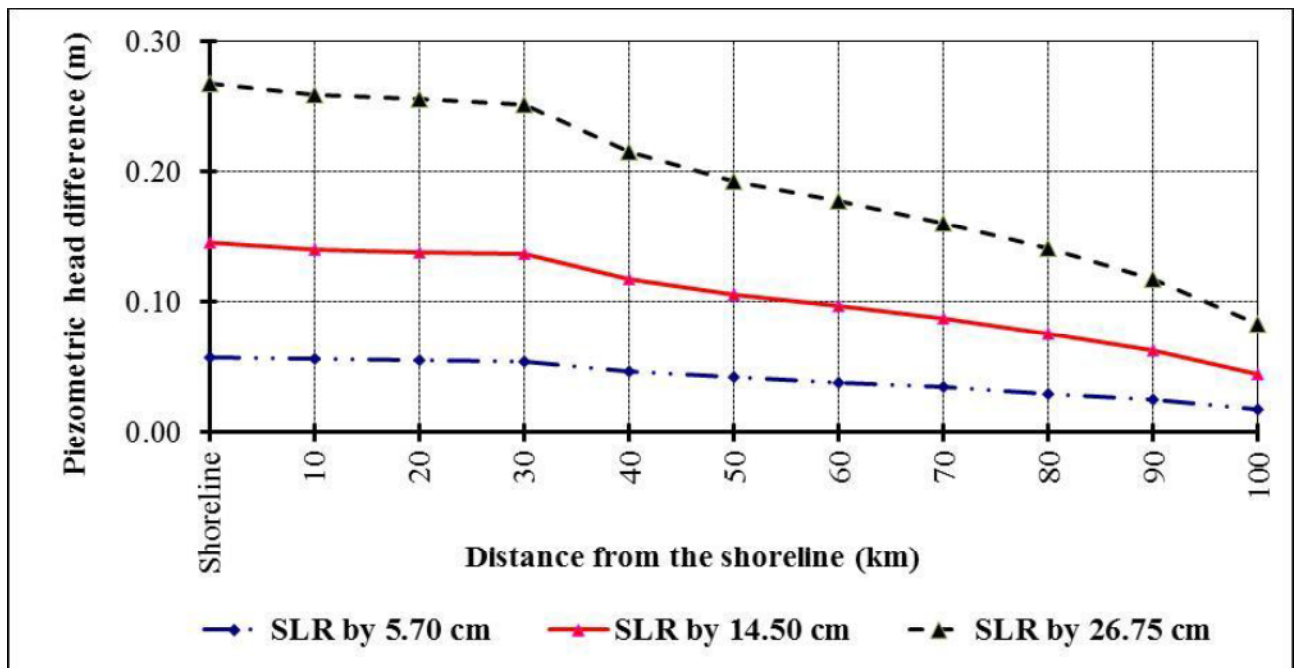
Time (year)	SLR (cm)	Recharge (%)	Intrusion length (km)		Aquifer salt variation $(C-C_0)/C_0$		Aquifer salt removal effect
			1000	35000	1000	35000	
2000	0	0	90.40	75.85	0	0	-

2020	5.7	0.50	90.37	75.87	+0.03	+0.02	negative
		<b>1</b>	<b>90.34</b>	<b>75.79</b>	<b>-0.07</b>	<b>-0.08</b>	positive
		1.50	90.30	75.72	-0.11	-0.17	positive
2040	14.5	1	90.39	75.90	-0.01	+0.06	negative
		<b>1.50</b>	<b>90.36</b>	<b>75.82</b>	<b>-0.04</b>	<b>-0.03</b>	positive
		2	90.33	75.75	-0.08	-0.13	positive
2060	26.7	2	90.4	75.90	0.00	+0.06	negative
		<b>3</b>	<b>90.34</b>	<b>75.75</b>	<b>-0.07</b>	<b>-0.13</b>	positive
		4	90.27	75.61	-0.14	-0.32	positive

385

386 It is clear that the three stages of SLR lead to increase groundwater level and SWI in the aquifer, as  
 387 expected. This rising would damage a relevant quantity of freshwater in the aquifer, increasing the salinity  
 388 of the soil and groundwater in the root zone.

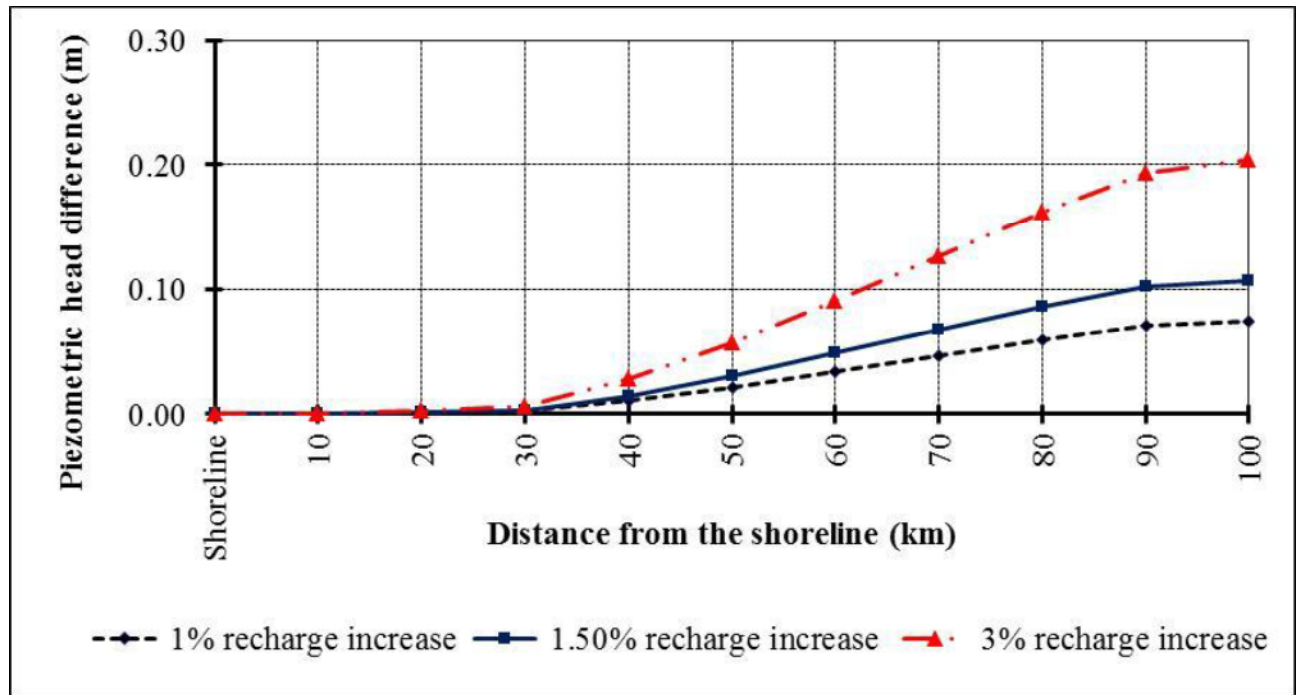
389 According to the model results, the control of SWI and soil salinity in the root zone under the  
 390 hypothesized SLR conditions (5.7 cm, 14.5 cm and 26.7 cm) would be performed by artificially  
 391 increasing the recharge by 1%, 1.5% and 3% respectively. This will lead to decrease SWI but increase  
 392 groundwater level. Figure 8 shows the relationship between piezometric head difference and the distance  
 393 from the shoreline under different SLR values and different scenarios of recharge. Figure 9 shows that the  
 394 maximum difference in head occurs at the South, due to the maximum values of recharge applied there.  
 395 The piezometric heads in the aquifer in the case study area under the different scenarios of recharge are  
 396 shown in Table 3, which will be fully discussed later in this paper.



397

398  
399

Figure 8: Relation between piezometric head difference and distance from the shoreline for the proposed scenarios of SLR



400

401 Figure 9: Relation between piezometric head difference (G) and distance from the shoreline according to  
402 the three proposed scenarios of SLR and recharge

### 403 3.2 The effect of subsidence on the coastal aquifer and its quantification

404 It is clear how a proper design of subsurface draining systems contributes to mitigate the vulnerability to  
405 climate change and to the increased anthropic pressure. The main parameters that have been considered  
406 until now are the sea level rise and the increased seepage from recharge. In the particular case of the Nile  
407 delta, it is important to analyse also the effect of subsidence on the estimation of flow into the drains. The  
408 expected mechanism by which subsidence may affect the sizing of the drains consists in the reduction of  
409 distance between the semi-confined and the phreatic layers, due to compaction of the volume in between,  
410 and, consequently, the hydraulic head gradient between them.

411 An estimation of the current subsidence rates can be based on recent literature, where the vertical land  
412 motion in the Nile delta coasts is measured by SAR interferometric techniques, by using the “persistent  
413 scatterer” (PS) approach (Wöppelmann et al, 2013; Becker & Sultan, 2009). Few algorithms have been  
414 developed, in order to extract the Line Of Sight (LOS) deformation from SARIn data, and subsequently  
415 the vertical component of such deformation. To probe deeper into this technology, the interested reader

416 may find relevant examples of said techniques in (Ferretti et al. 2001, Berardino et al. 2002, Hooper et al.  
417 2004).

418 Recent estimates of subsidence rates in the Nile delta are provided by Fugate (2014), very useful for the  
419 purpose of this paper even if mostly focused on the northwestern part of the delta. The work by  
420 Wöppelmann et al (2013) combined the InSAR acquisition with GPS measurements, with an interesting  
421 discussion of their relevant geodetic findings. The authors observed a very low rate of subsidence (about  
422 0.5 mm/yr) in the Alexandria coastal region, with a good agreement between InSAR PS technique and the  
423 tide gauge station in Alexandria. According to the authors, higher rates of about 5 mm/yr were observed  
424 in the northeastern part of the Nile delta. Becker and Sultan (2009) found subsidence rates up to 8 mm/yr  
425 in the northeastern coastal region, with relatively lower rates (4 to 6 mm/yr) around the Manzala lagoon.  
426 Fugate (2014) substantially confirmed these velocities, finding subsidence rates around 8 mm/yr with  
427 maximums about 10 mm/yr, in an area that covers a substantial part of the study area of this paper  
428 (Eastern Nile delta aquifer).

429 All authors observed high spatial variability of ground motion velocities, characterized by a very irregular  
430 spatial distribution, also in the presence of both uplift and subsidence phenomena in nearby zones.  
431 Despite that, a general trend to higher subsidence rates is clearly asserted for what regards the  
432 northeastern coastal region, with respect to the central and western ones. It is also important to underline  
433 here that the next filling of the GERD is expected to negatively affect vertical land motion velocities in  
434 the Nile delta, due to the lower water levels that will be experienced in the canals during the filling period  
435 and its possible direct geotechnical implication.

436 For the purpose of this paper, we assigned a constant subsidence rate of 8 mm/yr to the whole study area,  
437 as a cautious value to understand and better define the possible scenarios and their impact on the design  
438 of the drainage infrastructure. Table 3 in the next section shows the incremental contribution of  
439 subsidence to the flow into the SD system, combined with the other influencing factors (SLR and total  
440 recharge).

### 441 **3.3 Quantification of the impact on the subsurface drainage system design**

442 The previous sections demonstrated that the maximum increase of the piezometric head due to SLR  
443 occurs in the northern part of the study area, where the aquifer is directly connected with the sea. Also  
444 salinity experiences its maximum increase due to SLR on the northern coast, gradually decreasing toward  
445 the South. Given this spatial trend, Table 3 shows the values of the predicted piezometric heads ( $\Delta G$ ),  
446 calculated at a predetermined distance to the shore line (about 40 km) within the study area.

447 Given the foreseen increase of the piezometric heads, the impact of the increase of the piezometric heads  
448 ( $\Delta G$ ) on the SD performance could be calculated by using local scale numerical model described in  
449 section 2.2.2. More specifically, the subsurface drain discharge was calculated towards the predicted  
450 piezometric heads according to the different stressors, separately: i) SLR; ii) recharge increment and iii)  
451 subsidence. This has been done in order to make clear to the reader the importance of each contribution.

452 Figure 10 illustrates the hydraulic head distribution around the drains obtained with local numerical  
453 model, in the aquitard and in the phreatic aquifer in the given conditions. Table 3 summarises the  
454 simulation results for the proposed scenarios. In particular, the table shows the incremental contributions  
455 of SLR, recharge and subsidence to the flow into the SD system (named  $Q_{SLR}$ ,  $Q_R$  and  $Q_{Sub}$ , respectively).  
456 SLR values of 5.7 cm, 14.5 cm and 23.75 cm were respectively assigned to the years 2020, 2040 and  
457 2060, and entered in the numerical model (based on Eq. 1). As a consequence, piezometric heads due to  
458 SLR ( $\Delta G_{SLR}$ ) are calculated in 4.65, 11.70 and 21.50 cm, respectively. The estimated increment of  
459 discharge  $Q_{SLR}$  resulted about 0.81, 2.05 and 3.76 L/day·m for the three consecutive time horizons.

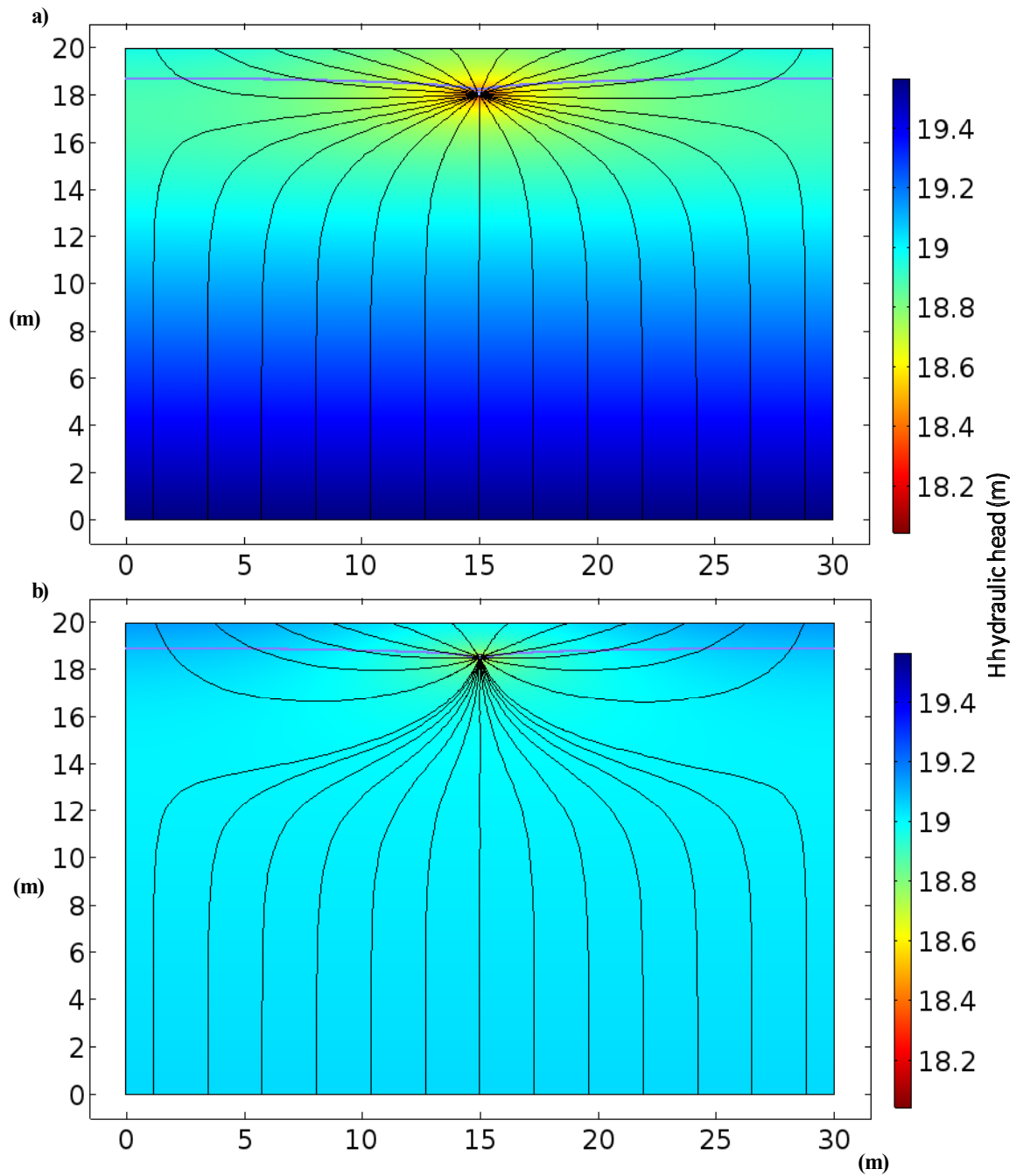


Figure 10: Water table (blue line), hydraulic head (false colors) and flow lines (black lines) around a drain. a) Scenario without SLR, Recharge and Subsidence (related to year 2000). b) Worst scenario with the maximum SLR, Recharge and Subsidence (year 2060).

460  
461  
462  
463  
464

465 When an increment of recharge is hypothesized towards increasing sea level scenarios, the discharge  
466 through the drains also increases, with an impact on the efficiency of the SD system that must be taken  
467 into account. Thus, further calculations of the model have been performed, inclusive of the additional  
468 input due to recharge, as described in Section 3.1. The increment of discharge  $Q_R$  through the SD system  
469 has been calculated in about 0.19, 0.26 and 0.49 L/day·m, corresponding to 1%, 1.5% and 3% of

470 recharge, which, in turn, increased the piezometric heads due to recharge ( $\Delta G_R$ ) to reach 1.10, 1.50 and  
 471 2.80 cm respectively (Table 3).

472 Finally, the role of subsidence has been quantified. In particular, the reduction of the distance (in terms of  
 473 depth below the soil level) between the SD and the hydraulic head was considered as a further input to the  
 474 model. As a result, additional discharge increments of 2.73, 5.74 and 8.69 L/day·m, corresponding to the  
 475 subsidence values assigned to the years 2020, 2040 and 2060, were obtained.

476 Considering all the inputs, the numerical findings show a total discharge increment of about 12.50%,  
 477 26.97% and 43.35% with respect to the initial Q. Thus, the inclusion of the scenarios studied in this paper  
 478 in a wider context of water resources management impacts the design of SD systems in a non-negligible  
 479 way, clearly indicated by the increasing discharge rates to be governed. This result is very relevant for the  
 480 water management of Nile delta area. In fact, the combination of multiple forcing parameters, such as  
 481 SLR, artificial subsurface recharge (made to reduce the aquifer salinity) and subsidence require a pre-  
 482 emptive action in the design and sizing of such fundamental hydraulic structures for the resiliency of  
 483 agriculture in the area under study.

484 **Table 3:** Summary of simulation results for the proposed scenarios. The impact on SD flow increment is  
 485 highlighted in bold

<b>Time (year)</b>	<b>2000</b>	<b>2020</b>	<b>2040</b>	<b>2060</b>
<b>Seal level rise (cm)</b>	0	5.7	14.5	26.7
<b><math>\Delta G_{SLR}</math> (cm)</b>	0	4.65	11.70	21.50
<b><math>Q_{SLR}</math> (L/day/m)</b>	0	0.81	2.05	3.76
<b>Recharge (%)</b>	0	1	1.5	3
<b><math>\Delta G_R</math> (cm)</b>	0	1.10	1.50	2.80
<b><math>Q_R</math> (L/day/m)</b>	0	0.19	0.26	0.49
<b><math>\Delta</math> Subsidence</b>	0	16	32	48
<b><math>Q_{Sub}</math> (L/day/m)</b>	0	2.73	5.74	8.69
<b><math>Q_{Total}</math> (L/day/m)</b>	29.84	3.73	8.05	12.94
<b><u>Variation of Q (%)</u></b>	<b>0</b>	<b>12.50</b>	<b>26.97</b>	<b>43.35</b>

486

#### 487 **4 Conclusions**

488 In this paper, the effect of climate-related drivers on the design of subsurface drainage systems in coastal  
489 aquifers is analysed by estimating the flow rate in the draining pipes and its possible increment due to  
490 hypothesized conditions of sea level rise, recharge and subsidence. Both surface and subsurface drainage  
491 networks in the northern part of the East Nile Delta were designed and realized in the past years, offering  
492 an exemplary study area for this research. The evaluations made in this paper are in terms of foreseen  
493 scenarios within a time horizon compatible with the life expectancy of the buried draining structure,  
494 taking year 2000 as a starting point and years 2020, 2040 and 2060 as reference years for the modelling  
495 exercise.

496 Regarding the climate change effects, the forcing parameters and their assigned values are briefly listed as  
497 follows:

- 498 i. Based on a “climate-change–driven” acceleration of  $0.084 \text{ mm/yr}^2$ , sea level rise values of  
499 5.7 cm, 14.5 cm and 26.7 cm (referred to year 2000) were estimated for the years 2020, 2040  
500 and 2060, respectively;
- 501 ii. An increment of artificial recharge in order to counteract the incremented sea water intrusion  
502 (thus, soil salinity in the root zone) is needed. The hypothesized sea level rise values (5.7 cm,  
503 14.5 cm and 26.7 cm) imply a recharge increment of about 1%, 1.5% and 3%, respectively;
- 504 iii. According to recent literature data, subsidence values of 16 cm, 32 cm and 48 cm (referred  
505 to year 2000) were calculated for the years 2020, 2040 and 2060, respectively;

506 Regarding the climate change impacts on the subsurface drainage system (i.e. the increment of flow rate)  
507 the outcome of our analyses are:

- 508 iv. For what regards the sea level rise, we estimated a discharge increment of about 0.81, 2.05  
509 and 3.76 L/day/m , corresponding to 5.7 cm, 14.5 cm and 23.75 cm of SLR, respectively;
- 510 v. For what regards the artificial recharge, a discharge increment of about 0.19, 0.26 and 0.49  
511 L/day/m was evaluated, corresponding to 1%, 1.5% and 3% of recharge, respectively;

- 512 vi. For what regards the subsidence, we estimated a discharge increment of about 2.73, 5.74 and  
513 8.69 L/day/m , corresponding to subsidence values of 16, 32 and 48 cm, respectively;
- 514 vii. Considering all the forcings (i.e., sea level rise, artificial recharge and subsidence), the  
515 numerical findings show a total discharge increment of about 3.73 L/day·m, 8.05 L/day·m  
516 and 12.94 L/day/m corresponding to a share of 12.50%, 26.97% and 43.35% with respect to  
517 the initial flow rate (year 2000).

518 This result is very relevant to the future groundwater management in the Nile delta area. In fact, the  
519 combination of multiple forcings, such as sea level rise, artificial subsurface recharge (for reducing the  
520 aquifer salinity) and subsidence, imply the need for region-specific action plans to minimize the effects of  
521 such stressors on the subsurface drainage system. In a wide context of water resources management, the  
522 design of subsurface drainage systems must take into account the effects of climate change as a  
523 fundamental component of the designing exercise. In particular, this paper demonstrates that the impact of  
524 the foreseen conditions on the discharge into the subsurface drainage systems is anything but negligible.

## 525 **References**

- 526 Abd-Elaty, I. M., Gehan.A.H.Sallam, Abdelaal, G. M., Eldin, O. W., (2010). Environmental Impact  
527 Assessment of Subsurface Drainage Projects in Egypt, the Egyptian International Journal of  
528 Engineering Science and Technology ,Vol. (13), No.(2), pp 411 – 418.  
529
- 530 Abd-Elaty, I. M., Abd-Elhamid H. F., Fahmy, M. R. and Abdelaal, G. M., (2014).” Investigation of some  
531 Potential Parameters and its Impacts on Saltwater Intrusion in Nile Delta Aquifer”, Journal of  
532 Engineering Sciences, Assiut University, Faculty of Engineering, Vol. (42), No. (4), PP 931-955.  
533
- 534 Abdel-Dayem, M. S. Y., (1984). Drain Spacing for falling water table in a clay cap over an artesian aquifer,  
535 PhD thesis, faculty of engineering, Cairo university, Egypt.  
536
- 537 Abd-Elhamid H., Javadi A., Abd-Elaty I., and Sherif M. (2016). Simulation of seawater intrusion in the Nile  
538 Delta aquifer under the conditions of climate change, Hydrology Research.  
539
- 540 Abd-Elhamid H. and Abd-Elaty I. (2017). Application of a new methodology (TRAD) to control seawater  
541 intrusion in the Nile delta aquifer, Egypt, Solutions to Water Challenges in MENA Region Proceedings  
542 of the Regional Workshop, April 25-30, 2017 - Cairo, Egypt.  
543
- 544 Abd-Elhamid H., Abd-Elaty I., & Sherif M. (2018). Evaluation of potential impact of Grand Ethiopian  
545 Renaissance Dam on Seawater Intrusion in the Nile Delta Aquifer. International Journal of  
546 Environmental Science and Technology, pp. 1-12.  
547
- 548 Aboel Ghar M., Shalaby A. & Tateishi R. (2004). Agricultural land monitoring in the Egyptian Nile Delta  
549 using Landsat data. International Journal of Environmental Studies, 61(6), 651-657, DOI:  
550 10.1080/0020723042000253866.

551  
552 Abu-Zied, M., and Abdel-Dayem, G. (1991) Soil load in irrigation and drainage water in the Nile Delta, In:  
553 African Regional Symposium on Techniques for environmentally sound water resources Development.  
554  
555 Agren J., Svensson R. (2007). Postglacial Land Uplift Model and System Definition for the New Swedish  
556 Height System RG 2000; Lantmäteriet: Gävle, Sweden.  
557  
558 Amer, A.M., (1981). Physics of the Nile Delta Aquifer. Proceedings of International Workshop on  
559 Management of the Nile Delta Groundwater Aquifer, Cairo University, Giza, Egypt.  
560  
561 Atta A. S. (1979). Studies on the groundwater properties of the Nile Delta, Egypt, M.Sc. Thesis, Fac. of Sc.,  
562 Cairo University, 311–325.  
563  
564 Bazaraa A. S., Abdel-Dayem M. S, Amer A., and Willardson L. S., (1986). Artesian and Anisotropic Effects  
565 on Drain Spacing, Journal of Irrigation and Drainage Engineering, Vol. 112, No. 1, February 1986, pp.  
566 55-64.  
567  
568 Becker, R. H., & Sultan, M. (2009). Land subsidence in the Nile Delta: inferences from radar interferometry.  
569 The Holocene, 19(6), 949-954.  
570  
571 Berardino, P., Fornaro, G., Lanari, R., & Sansosti, E. (2002). A new algorithm for surface deformation  
572 monitoring based on small baseline differential SAR interferograms. IEEE Transactions on Geoscience  
573 and Remote Sensing, 40(11), 2375-2383.  
574  
575 British Columbia Agriculture & Food Climate Action Initiative (2013) BC Farm Practices & Climate  
576 Change Adaptation series: Drainage, [www.BCAGClimateAction.ca](http://www.BCAGClimateAction.ca).  
577  
578 COMSOL Multiphysics (2008). User's guide version 3.5, Stockholm.  
579  
580 Crosetto M., Monserrat O., Cuevas-González M., Devanthéry N. & Crippa B. (2016). Persistent scatterer  
581 interferometry: A review. ISPRS Journal of Photogrammetry and Remote Sensing, 115, 78-89.  
582  
583 Deelstra J. (2015) Climate change and subsurface drainage design: results from a small fieldscale catchment  
584 in south-western Norway, Acta Agriculturae Scandinavica, Section B — Soil & Plant Science, 65:sup1,  
585 58-65, DOI: 10.1080/09064710.2014.975836  
586  
587 El-Fayoumi, F., (1987). Geology of the Quaternary Succession and Its Impact on the Groundwater Reservoir  
588 in the Nile Delta Region, Bull. Fac. Sci., Menofia Univ., Egypt.  
589  
590 El Raey M., (2010) Impact and Implications of Climate Change for the Coastal Zones of Egypt. In: Michel,  
591 D., Pandya, A. (eds.) (2010), Coastal Zones and Climate Change.  
592  
593 ESA SL-CCI (2018) <http://www.esa-sealevel-cci.org/node/248>, accessed 19 June 2018.  
594  
595 Essink K. and Kleef H. L.(1993). Distribution and life cycle of the North American spionid polychaete  
596 *Marenzelleria viridis* (verrill,1873) in the Ems estuary, edited by: Meire, P. and Vincx, M., 1993.  
597  
598 Fawzi I., Kamel M.S. (1994). Design of drainage system, design criteria adopted by EPADP. Refreshing  
599 course on land drainage in Egypt, 10-19 December 1994.  
600  
601 Faried M. S., (1979). Nile delttta groundwaer study, unpublished M. Sc. thesis, Faculty of Engineering, Cairo  
602 University, Giza, Egypt.  
603

- 604 Farid M.S.M. (1980) Nile Delta Groundwater Study, M.Sc. Thesis, Cairo University.  
605
- 606 Farid M.S.M. (1985) Management of groundwater systems in the Nile Delta. PhD Thesis, Cairo Univ., Giza,  
607 Egypt.  
608
- 609 Ferretti A., Prati C., & Rocca F. (2001). Permanent scatterers in SAR interferometry. IEEE Transactions on  
610 geoscience and remote sensing, 39(1), 8-20.  
611
- 612 Fugate J. M. (2014). Measurements of land subsidence rates on the northwestern portion of the Nile Delta  
613 using radar interferometry techniques (M. Sc. Thesis).  
614
- 615 Hooper A., Zebker H., Segall P., & Kampes B. (2004). A new method for measuring deformation on  
616 volcanoes and other natural terrains using InSAR persistent scatterers. Geophysical research letters,  
617 31(23).  
618
- 619 IPCC (2008). Climate Change and Water, Technical Paper of the Intergovernmental Panel on Climate  
620 Change, edited by: Bates, B. C., Kundzewicz, Z. W., Wu, S., and Palutikof, J. P., IPCC Secretariat,  
621 Geneva, p. 210.  
622
- 623 IPCC (2013): Climate Change 2013: The Physical Science Basis. Contribution of Working Group I to the  
624 Fifth Assessment Report of the Intergovernmental Panel on Climate Change [Stocker, T.F., D. Qin, G.-  
625 K. Plattner, M. Tignor, S.K. Allen, J. Boschung, A. Nauels, Y. Xia, V. Bex and P.M. Midgley (eds.)].  
626 Cambridge University Press, Cambridge, United Kingdom and New York, NY, USA, 1535 pp.  
627
- 628 Kalantari Z. (2011). Adaptation of Road Drainage Structures to Climate Change, TRITA LWR LIC 2061  
629
- 630 Langevin C.D., Thorne D.T. Jr., Dausman A.M., Sukop M.C., and Guo Weixing (2008). SEAWAT Version  
631 4: A computer program for simulation of multi-species solute and heat transport: U.S. Geological  
632 Survey Techniques and Methods, book 6, chap. A22, 39 p.  
633
- 634 Laeven M.T. (1991). Hydrogeological study of the Nile Delta and adjacent desert areas, Egypt, with  
635 emphasis on hydrochemistry and isotope hydrology, M.Sc. thesis, Free University, Amsterdam. Also  
636 published by RIGW/IWACO as Technical Note TN 77.01300-91-01.  
637
- 638 Legeais J.-F., Ablain M., Zawadzki L., Zuo H., Johannessen J. A., Scharffenberg M. G., Fenoglio-Marc L.,  
639 Fernandes M. J., Andersen O. B., Rudenko S., Cipollini P., Quartly G. D., Passaro M., Cazenave A.,  
640 and Benveniste J. (2018). An improved and homogeneous altimeter sea level record from the ESA  
641 Climate Change Initiative, Earth Syst. Sci. Data, 10, 281-301, [https://doi.org/10.5194/essd-10-281-  
642 2018](https://doi.org/10.5194/essd-10-281-2018).  
643
- 644 Morsy W. S. (2009). Environmental management to groundwater resources for Nile delta Region, PhD  
645 thesis, Faculty of Engineering, Cairo University, Egypt.  
646
- 647 Nerem R. S., Beckley B. D., Fasullo J. T., Hamlington B. D., Masters D., & Mitchum G. T. (2018). Climate-  
648 change-driven accelerated sea-level rise detected in the altimeter era. Proceedings of the National  
649 Academy of Sciences, 201717312, doi:10.1073/pnas.1717312115.  
650
- 651 Nosair A. M. (2011). Climate changes and their impacts on groundwater occurrence in the northern part of  
652 East Nile delta, M.Sc. Thesis, Faculty of Science, Zagazig University, Egypt.  
653
- 654 MWRI (2013). Proposed climate change adaptation strategy for the Ministry of Water Resources and  
655 Irrigation (MWRI) in Egypt, tech. report, Ministry of Water Resources and Irrigation, Egypt.  
656

- 657 Pease L.A., Fausey N.R., Martin J.F., and Brown L.C.(2017). Projected climate change effects on subsurface  
658 drainage and the performance of controlled drainage in the Western Lake Erie Basin, *Journal of Soil and*  
659 *Water Conservation*, Vol. (72), No. 3.
- 660
- 661 RIGW/IWACO (1990). Development and management of groundwater resources in the Nile Valley and  
662 Delta: Assessment of groundwater pollution from agricultural activities, Internal report, Research  
663 Institute for Groundwater, El Kanater El Khairia, Egypt.
- 664
- 665 RIGW (Research Institute for Groundwater) (1980) Projected of the Safe Yield Study for Groundwater  
666 Aquifer in the Nile Delta and Upper Egypt, part 1 (in Arabic). Ministry of Irrigation, Academy of  
667 Scientific Research and Technology, and Organization of Atomic Energy, Egypt.
- 668
- 669 RIGW (2002). Nile Delta Groundwater Modeling Report. Research Inst. for Groundwater, Kanater El-  
670 Khairia, Egypt.
- 671
- 672 Said, R. (1962) *The Geology of Egypt*. Elsevier Publishing Company, Amsterdam, New York, 377 pp.
- 673
- 674 Said, R. (1981). *The Geological Evolution of the River Nile*. Springer-Verlag, New York, 151 pp.
- 675
- 676 Said, R., (1993). *The Nile River: Geology, Hydrology, and Utilization*. Pergamon, New York, USA, 320 pp.
- 677
- 678 Sakr S. A., Attia F. A., and Millette J. A. (2004). Vulnerability of the Nile Delta aquifer of Egypt to seawater  
679 intrusion, International conference on water resources of arid and semi-arid regions of Africa, Issues and  
680 challenges, Gaborone, Botswana.
- 681
- 682 Sallam O., M., (2018) Vision for Future Management of Groundwater in the Nile Delta of Egypt After  
683 Construction of the Ethiopian Dams, *Hydrology: Current Research*, Vol (9), Issue (3).
- 684
- 685 Serag EI-Din, H., 1989. Geological, Hydrogeological and Hydrological Studies on the Quaternary Aquifer,  
686 Egypt, PhD Dissertation, Mansoura Univ., Egypt.
- 687
- 688 Sestini G.(1989). Nile Delta: A review of depositional environments and geological history.  
689 In Whateley, M.K.G. and Pickering, K.T. eds. : *Deltas : Sites and Traps for Fossil Fuels*. Geol.  
690 Soc. Spec. Publ., 41, 99-127.
- 691
- 692 Shaltout M., Tonbol K., and Omstedt A. (2015). Sea-level change and projected future flooding along the  
693 Egyptian Mediterranean coast, *Oceanologia*, v. 57, p. 293–307, doi: 10.1016/ j.oceano.2015.06.004.
- 694
- 695 Sherif M. M and Al-Rashed M. F. (2001). Vertical and Horizontal Simulation of Seawater Intrusion in the  
696 Nile Delta Aquifer, Proceeding of the 1st International Conference and Workshop on Saltwater  
697 Intrusion and Coastal Aquifers, Monitoring, Modelling, and Management (Morocco).
- 698
- 699 Sherif M.M., Sefelnasr A., and Javadi A. (2012). Incorporating the concept of equivalent freshwater head in  
700 successive horizontal simulations of seawater intrusion in the Nile Delta Aquifer, Egypt. *Journal of*  
701 *Hydrology* 464–465: 186–198. DOI: org/10.1016/ j.jhydrol.2012.07.007.
- 702
- 703 Sefelnasr. A. and Sherif M., (2014). Impacts of Seawater Rise on Seawater Intrusion in the Nile Delta  
704 Aquifer, Egypt, *Groundwater Journal*, Vol. (52), No.(2), p. 264–276.
- 705
- 706 Stanley, J.-D., and Corwin, K. A. (2012) Measuring Strata Thicknesses in Cores to Assess Recent Sediment  
707 Compaction and Subsidence of Egypt's Nile Delta Coastal Margin: *Journal of Coastal Research*  
708

- 709 Vignudelli S., Kostianoy A.G., Cipollini P., Benveniste J. (Eds) (2011). Coastal Altimetry, Springer-Verlag  
710 Berlin Heidelberg, pp. 19-50, doi:10.1007/978-3-642-12796-0\_19  
711
- 712 Wöppelmann G., Le Cozannet G., De Michele M., Raucoules D., Cazenave A., Garcin M., ... &  
713 Santamaría-Gómez A. (2013). Is land subsidence increasing the exposure to sea level rise in  
714 Alexandria, Egypt? *Geophysical Research Letters*, 40(12), 2953-2957.